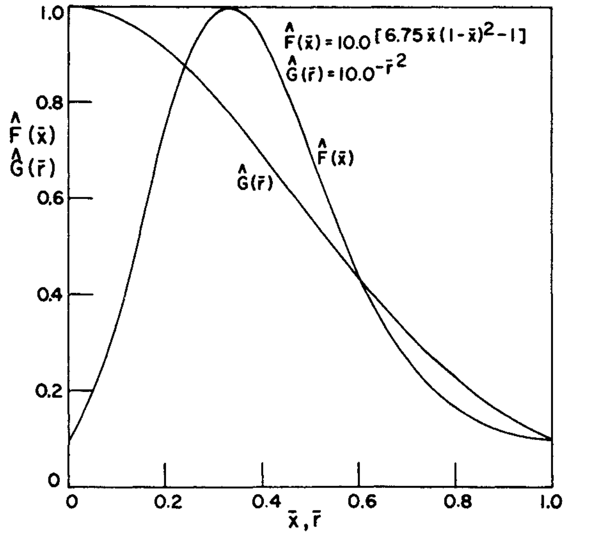

Fig. 1 Longitudinal and lateral distributions of pressure source in a turbulent jet.

and the nozzle diameter D. Thus the longitudinal source distribution can be adequately represented by the expression

$$\frac{\log p/p_1}{(\log p/p_i)_{\max}} = \frac{27}{4}\bar{x}(1-\bar{x})^2 \tag{5}$$

where the nondimensional distance $\bar{x}$ is now equal to $(St\,x/D)/l$, l is the extent of the source distribution in terms of the normalized distance and is approximately equal to 3.0 (Ref. 3). Thus the source function $\hat{F}(\bar{x})$ can be written as

$$\hat{F}(\bar{x}) = C_2^{[(27/4)\bar{x}(1-\bar{x})^2-1]} \tag{6}$$

with $C_2 = 10.0$ and $\bar{x}$ ranges from zero to unity.

The lateral source distributions can be represented by the expression

$$\frac{\log p/p_1}{(\log p/p_1)_{\max}} = 1-\bar{r}^2 \tag{7}$$

Since the jet spreads out laterally downstream from the nozzle, the lateral dimension of the source, R, is not a constant. However, in evaluating the integral a mean value of R can be taken and the source function can thus be written as

$$\hat{G}(\bar{r}) = C_2^{-\bar{r}^2} \tag{8}$$

The functions $\hat{F}(\bar{x})$ and $\hat{G}(\bar{r})$ are shown graphically in Fig. 1.

The source integrals, I_x and I_r, for the symmetric case ($m = 0$) are evaluated numerically for the source functions given in Eqs. (6) and (8) and the results are shown in Fig. 2. Figure 3 shows the squares of the amplitude of the source integrals, the

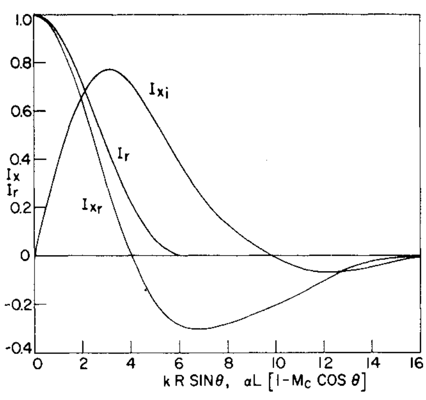

Fig. 2 Real and imaginary parts of the longitudinal source integral, I_{x_r}, I_{x_i} vs $\alpha L[1-M_c\cos\theta]$ and the lateral source integral I_r vs $kR\sin\theta$.

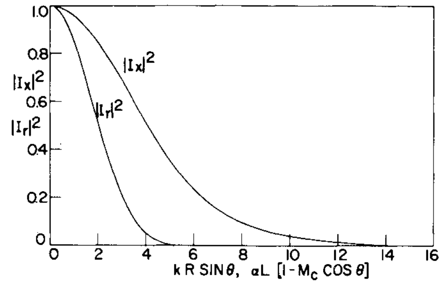

Fig. 3 Squares of the amplitude of the longitudinal source integral $|I_x|^2$ vs $\alpha L[1-M_c\cos\theta]$ and the lateral source integral $|I_r|^2$ vs $kR\sin\theta$.

product of which is proportional to the far field sound intensity. It is interesting to point out that model (IV) for the longitudinal source and model (b) for the lateral distribution assumed by Michalke (see Figs. 1 and 3 of Ref. 4) are closely similar to the present results derived from experimental data.

The present forms of the source integrals can now be used for the calculation of the axisymmetric component of the far field sound intensity based on the wave-model formulation. Because the axisymmetric component of the source term radiates much more sound than the asymmetric components, the calculated results based on the present source integrals will be a good approximation to the total sound intensity radiated by the turbulent jet.

References

[1] Mollφ-Christensen, E., "Jet Noise and Shear Flow Instability seen from an Experimenter's Viewpoint," *Journal of Applied Mechanics*, Vol. 34, 1967, pp. 1–7.

[2] Crow, S. C. and Champagne, F. H., "Orderly Structure in Jet Turbulence," *Journal of Fluid Mechanics*, Vol. 48, Pt. 3, 1971, pp. 547–591.

[3] Chan, Y. Y., "Spatial Waves in Turbulent Jets," *The Physics of Fluids*, Vol. 17, No. 1, Jan. 1974.

[4] Michalke, A., "A Wave Model for Sound Generation in Circular Jets," *Deutsche Luft-und Raumfahrt*, FB 70-57, 1970.

[5] Michalke, A., "An Expansion Scheme for the Noise from Circular Jets," *Zeitschrift für Flugwissenschaften*, Vol. 20, Heft 6, 1972, pp. 229–237.

[6] Ribner, H. S., "Aerodynamic Sound from Fluid Dilatations," UTIA Rept. 86, AFOSRTN 3430, July 1962, Inst. of Aerophysics, Univ. of Toronto, Toronto, Ontario, Canada.

Attachment-Line Flow on an Infinite Swept Wing

TUNCER CEBECI*
Douglas Aircraft Company, Long Beach, Calif.

Introduction

RECENTLY the present author developed a general method for calculating three-dimensional incompressible laminar, transitional, and turbulent boundary layers and investigated its accuracy for infinite swept wings.[1] The method uses the eddy-viscosity concept to model the Reynolds shear-stress term. The calculated results agreed well with experiment and with those results obtained by Bradshaw's method. In this Note, we shall

Received July 25, 1973; revision received October 5, 1973. This work was supported by the NASA Contract NAS1-11623.

Index category: Boundary Layers and Convective Heat Transfer—Turbulent.

* Manager, Viscous Flows Research Section. Member AIAA.

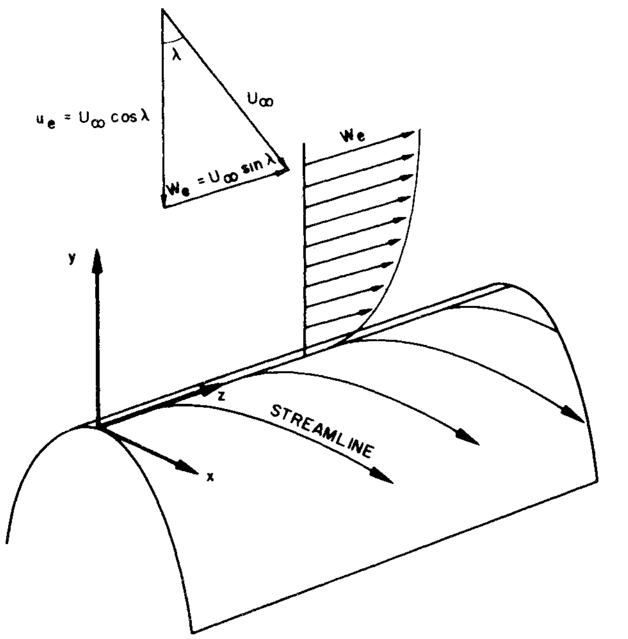

Fig. 1 Sketch of potential-flow streamline in attachment-line region of an infinite swept wing and the coordinate system.

investigate the accuracy of that method for an incompressible attachment line flow on an infinite swept wing.

Figure 1 shows a sketch of potential flow streamlines in the attachment-line region of an infinite swept wing, together with the rectangular coordinate system that will be used in this Note. The parameter that determines whether the flow will be laminar or turbulent is a dimensionless parameter defined by

$$C^* = w_e^2(du_e/dx)^{-1}\nu^{-1} \tag{1}$$

It may be regarded as a Reynolds number with the length scale represented by the ratio of spanwise velocity, w_e, to chordwise velocity gradient, du_e/dx. According to the experiments of Cumpsty and Head,[2] flow along the leading edge is fully turbulent for $C^* > 1.4 \times 10^5$. For $C^* < 0.8 \times 10^5$, the flow is laminar. In the range $0.8 \times 10^5 < C^* < 1.4 \times 10^5$, the flow is transitional.

Governing Boundary-Layer Equations

The governing boundary-layer equations for an incompressible turbulent flow past a yawed infinite wing, with the use of eddy-viscosity concepts, can be written as

Continuity

$$\partial u/\partial x + \partial v/\partial y = 0 \tag{2}$$

Chordwise Momentum

$$u\,\partial u/\partial x + v\,\partial u/\partial y = -(1/\rho)(dp/dx) + \nu\,\partial/\partial y[(1+\varepsilon^+)\,\partial u/\partial y] \tag{3}$$

Spanwise Momentum

$$u\,\partial w/\partial x + v\,\partial w/\partial y = (\partial/\partial y)[(1+\varepsilon^+)\,\partial w/\partial y] \tag{4}$$

On the attachment line, $u \equiv 0$. Therefore, Eq. (3) is singular along the line (leading edge) $x = 0$. To remove the singularity, we differentiate Eq. (3) with respect to x and set u and $\partial v/\partial x$ equal to zero. That procedure together with the use of Bernoulli's equation, $-1/\rho\, d^2p/dx^2 = (du_e/dx)^2$, enables Eq. (3) to be written as $[u_x \equiv \partial u/\partial x,\ B \equiv (du_e/dx)_{x=0}]$

$$u_x^2 + v\,\partial u_x/\partial y = B^2 + \nu\,\partial/\partial y[(1+\varepsilon^+)\,\partial u_x/\partial y] \tag{5}$$

If we now define

$$f'(\eta) = \lim_{x\to 0} u/u_e = (du/dx)(du_e/dx)^{-1}, \quad \eta = (B/\nu)^{1/2}y \tag{6}$$

then we can integrate Eq. (2) to get

$$v = -(B\nu)^{1/2}f \tag{7}$$

With the use of Eq. (7), it can be shown that the two momentum equations (4) and (5) can be written as

$$(bf'')' + ff'' + 1 - (f')^2 = 0 \tag{8}$$

$$(bg'')' + fg'' = 0 \tag{9}$$

where $b \equiv 1 + \varepsilon^+$, $g' \equiv w/w_e$.

Equations (8) and (9) are subject to the following boundary conditions:

$$\eta = 0 \quad f = 0 \quad \text{Or} \quad -v_w/w_e(C^*)^{1/2}\ (\text{mass transfer}), \quad f' = g = g' = 0 \tag{10a}$$

$$\eta = \eta_\infty \quad f' = g' = 1 \tag{10b}$$

Eddy Viscosity Formulation

According to the eddy viscosity formulation of Ref. 1, we define

$$\varepsilon \equiv \begin{cases} \varepsilon_i = (\kappa y)^2[1-\exp(-y/A)]^2|\partial w/\partial y| & 0 \leq y \leq y_c \\ \varepsilon_0 = \alpha\left|\int_0^\infty (w_e - w)\,dy\right| & y_c \leq y \leq \delta \end{cases} \tag{11}$$

where $\kappa = 0.4$, $\alpha = 0.0168$ and A is a damping-length constant. For a zero-pressure gradient flow with no mass transfer, it is given by $(A^+ = 26)$

$$A = A^+\nu(\tau_w/\rho)^{-1/2}$$

In terms of transformed variables, Eq. (11) can be written as

$$\varepsilon^+ = \begin{cases} \varepsilon_i^+ = \kappa^2(C^*)^{1/2}\eta^2|g''|\left[1-\exp\left(-\dfrac{\eta|g_w''|^{1/2}(C^*)^{1/4}}{A^+}\right)\right]^2 \\ \varepsilon_0^+ = \alpha(C^*)^{1/2}[\eta_\infty - g_\infty] \end{cases} \tag{12}$$

In the study reported here, we have used Eq. (12) to compute the fully turbulent boundary layers ($C^* > 1.4 \times 10^5$) on the leading edge of an infinite swept wing. The two momentum equations, Eqs. (8) and (9), were solved by using the numerical method of Ref. 3.

When several runs were made for different values of C^*, the solutions indicated very strong oscillations. The oscillations were small at small values of C^*, but they became quite strong at high values of C^*. It should be pointed out that such oscillations are not unusual in turbulent boundary-layer calculations. The appearance of such oscillations arise as a result of the inner eddy-viscosity formula (ε_i) given in Eq. (11); they are observed in all numerical methods that use this formula. However, the oscillations in nonsimilar turbulent flows are quite small and have no bearing on the accuracy of the solutions.

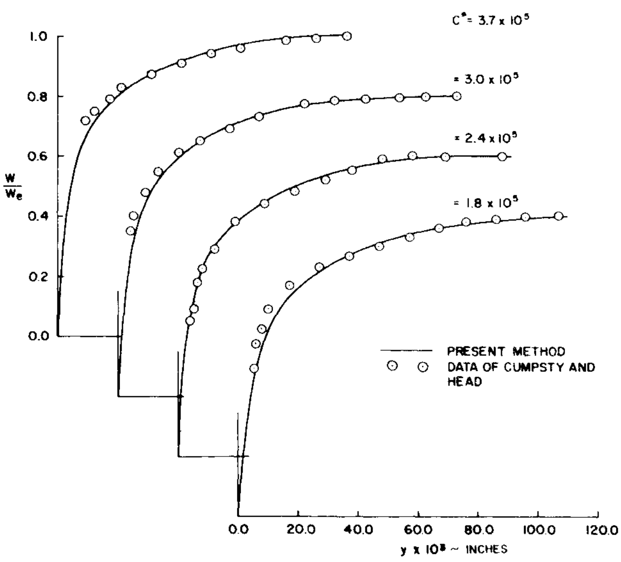

Fig. 2 Comparison of computed and experimental velocity profiles for the fully turbulent, attachment-line flow.

In order to eliminate the oscillations and provide convergence, we have replaced the inner-eddy-viscosity formula ε_i by

$$\varepsilon_i = \kappa y^+[1-\exp(-y/A)]\nu \tag{13}$$

which, in terms of transformed variables, can be written as

$$\varepsilon_i^+ = \kappa\eta(g_w''C^*)^{1/2}\left[1-\exp\left(-\frac{\eta|g_w''|^{1/2}|(C^*)^{1/4}}{A^+}\right)\right] \tag{14}$$

With that change, no oscillations were observed, and the solutions converged quadratically for all values of C^* considered.

Comparison with Experiment

Detailed measurements of attachment-line flows in turbulent boundary layers in incompressible flows are lacking in the literature. The only detailed data known to this author are the data of Cumpsty and Head.[2] For this reason, the present calculations are limited to that data. Figure 2 shows computed and experimental velocity profiles for four values of C^*.

As was mentioned before, the flow is fully turbulent only when $C^* > 1.4\times10^5$. For the range of $0.8\times10^5 < C^* < 1.4\times10^5$, the flow is transitional. The calculation for that region was extended by using the intermittency factor γ_{tr} used by Cebeci.[4] For an incompressible flow with zero pressure gradient, it is given by

$$\gamma_{tr} = 1-\exp\left[-G\left(\frac{x-x_{tr}}{w_e}\right)^2\right] \tag{15}$$

where G is

$$G = 0.835\times10^{-3}(w_e^3/\nu^2)R_{x_{tr}}^{-1.34} \tag{16}$$

To have similarity, we have written Eq. (15) as

$$\gamma_{tr} = 1-\exp(-Gx_{tr}^2/w_e)$$

which, with the use of Eq. (16), can also be written as

$$\gamma_{tr} = 1-\exp[-0.835\times10^{-3}(R_x)^{0.66}] \tag{17}$$

According to a recent study by Bushnell and Alston,[5] in calculating transitional boundary layers it is also necessary to account for the low Reynolds number effect (if there is one) in addition to the intermittent behavior of the flow. Here we account for this effect by expressing κ and A^+ as functions of Reynolds number[6]

$$\kappa = 0.40+[0.19/(1+0.49Z_2^2)],\quad A^+ = 26+[14/(1+Z_2^2)] \tag{18}$$

where $Z_2 = R_\theta\times10^{-3} > 0.3$. We also express α as a function of Reynolds number[7]

$$\alpha = 0.0168[1.55/(1+\Pi)] \tag{19}$$

where

$$\Pi = 0.55[1-\exp(-0.243Z_1^{1/2}-0.298Z_1)],\quad Z_1 = R_\theta/425-1$$

An examination of the experimental data of Cumpsty and Head shows that for the range of $0.8\times10^5 < C^* < 1.4\times10^5$, the Reynolds number based on θ, R_θ, varies between 200 and 400. Now the correction to α in Eq. (19) applies for R_θ greater than 425. For lower R_θ values, we simply extrapolate that curve as shown in Fig. 3 with a dashed line. The resulting (α, R)-curve can be approximated by the following formula:

$$\alpha\times10^3 = 194.8-128.6(\log_{10}R_\theta)+30.925(\log_{10}R_\theta)^2-2.475(\log_{10}R_\theta)^3$$

for $10^2 < R_\theta < 10^4$.

Figure 4 shows the calculated transitional boundary-layer profiles, together with the experimental data of Cumpsty and Head.[2] Figure 5 shows a comparison between calculated and measured local skin-friction values. Again the agreement with experiment is satisfactory.

Finally, we present the computed R_θ and H-values in Table 1 at different C^*-values. We also present the experimental R_θ-values given by Cumpsty and Head.

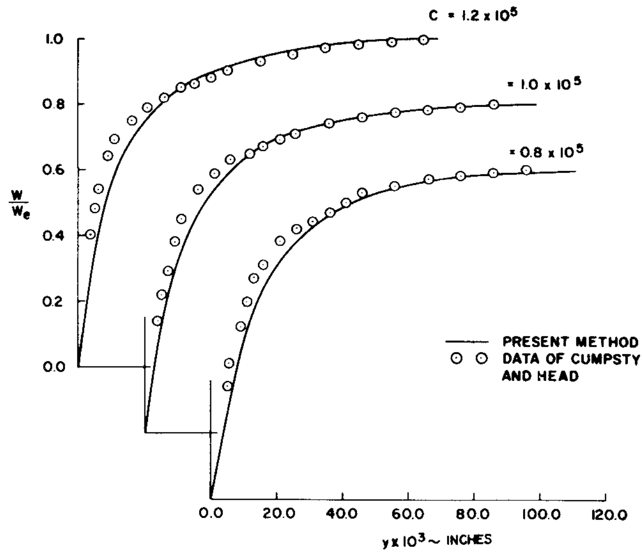

Fig. 4 Comparison of computed and experimental velocity profiles for the transitional attachment-line flow.

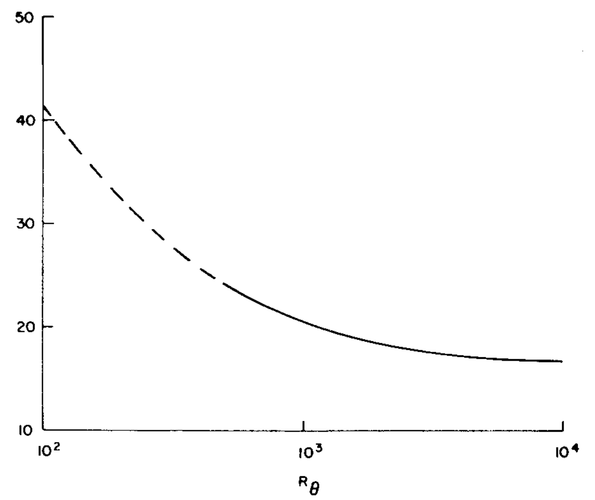

Fig. 3 Variation of α with Reynolds number.

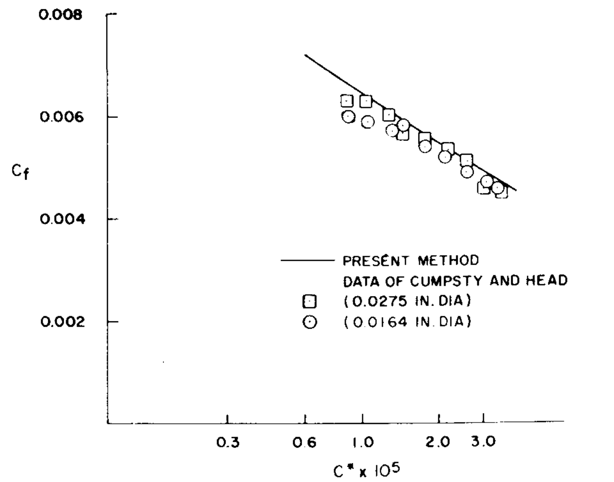

Fig. 5 Comparison of computed and experimental skin-friction values for the attachment-line flow.

References

[1] Cebeci, T., "A General Method for Calculating Three-Dimensional Incompressible Laminar and Turbulent Boundary Layers. I. Swept Infinite Cylinders and Small Cross Flow," *AIAA Journal*, to be published.

Table 1 R_θ and H-values for various C^*-values

	Exp.	Computed	
$C^* \times 10^{-5}$	R_θ	R_θ	H
0.8	200	225	1.76
1.0	250	270	1.71
1.2	295	313	1.68
1.8	430	434	1.60
2.4	540	538	1.57
3.0	640	634	1.55
3.7	760	735	1.53

[2] Cumpsty, N. A. and Head, M. R., "The Calculation of the Three-Dimensional Turbulent Boundary Layer. Part 3. Comparison of Attachment-Line Calculations with Experiment," *The Aeronautical Quarterly*, Vol. 20, May 1969, pp. 99–113.

[3] Keller, H. B. and Cebeci, T., "Simple Accurate Numerical Methods for Boundary Layers. II. Two-Dimensional Turbulent Flows," *AIAA Journal*, Vol. 10, No. 9, Sept. 1972, pp. 1197–1200.

[4] Cebeci, T., "Wall Curvature and Transition Effects in Turbulent Boundary Layers," *AIAA Journal*, Vol. 9, No. 9, Sept. 1971, pp. 1868–1870.

[5] Bushnell, D. M. and Alston, D. W., "On the Calculation of Transitional Boundary Layers," *AIAA Journal*, Vol. 11, No. 4, April 1973, pp. 554–556.

[6] Cebeci, T. and Mosinskis, G. J., "Computation of Incompressible Turbulent Boundary Layers at Low Reynolds Numbers," *AIAA Journal*, Vol. 9, No. 8, Aug. 1971, pp. 1632–1634.

[7] Cebeci, T., "Kinematic Eddy Viscosity at Low Reynolds Numbers," *AIAA Journal*, Vol. 11, No. 1, Jan. 1973, p. 102.

Comments on Crocco's Solution and the Independence Principle for Compressible Turbulent Boundary Layers

IVAN E. BECKWITH*
NASA Langley Research Center, Hampton, Va.

Nomenclature†

F = $\bar{F}+F' = \bar{u}/u_e + u'/u_e$, instantaneous chordwise velocity profile
g = $\bar{g}+g' = \bar{w}/w_e + w'/w_e$, instantaneous spanwise velocity profile
h = static enthalpy
H = $h+(u^2+v^2+w^2)/2$, total enthalpy
m = mass flow
M = Mach number
p = pressure
Pr = molecular Prandtl number
q = $(u^2+v^2+w^2)^{1/2}$
R_δ = local Reynolds number based on boundary-layer thickness, $\rho_e u_e \delta/\mu_e$
t = time
u = velocity parallel to surface in x-direction (chordwise component)
v = velocity normal to surface
$\tilde{v}$ = $\bar{v}+\overline{\rho' v'}/\rho$
w = velocity parallel to surface in z-direction (spanwise component)
x = distance along surface normal to cylinder generators (chordwise coordinate)
y = distance normal to surface
z = distance along surface parallel to cylinder generators (spanwise coordinate)
γ = ratio of specific heats
δ = boundary-layer thickness
μ = viscosity coefficient
ρ = mass density
θ = $\bar{\theta}+\theta' = \dfrac{\bar{H}-H_w}{H_e-H_w}+\dfrac{H'}{H_e-H_w}$, instantaneous total enthalpy profile

Subscripts

e = local freestream
w = wall conditions

Symbols

$(\bar{\ })$ = time mean quantity
$(\ )'$ = fluctuating quantity
$\sim$ = order of magnitude
$\approx$ = approximately equal

Received July 24, 1973.
Index categories: Boundary Layers and Convective Heat Transfer—Turbulent; Supersonic and Hypersonic Flow.
* Head, Gas Dynamics Section, Hypersonic Vehicles Division. Associate Fellow AIAA.
† All local variables without either an overbar or superscript prime are the instantaneous values.

Introduction

IT has been recognized[1] for many years that Crocco's solution[2] to the energy equation for the compressible laminar boundary layer on a flat plate applies to turbulent flow if both the molecular and turbulent Prandtl numbers are unity. Schaubauer and Tchen[3] showed further if the mean flow is exactly parallel, the only requirement for the applicability of the Crocco solution ($\bar{\theta} = \bar{F}$) to turbulent flow is that the molecular Prandtl number is unity. Thus, when the limitations of zero streamwise pressure gradient, molecular Prandtl number unity, turbulent Prandtl number unity, and/or parallel flow are nearly satisfied, the Crocco solution provides a useful approximation to the temperature distribution across turbulent boundary layers.[4,5] Another limitation, not usually considered, is that the wall temperature should be constant.[6] Recent results obtained by Feller[7] have shown that the relation between the normalized total temperature and velocity profile parameters is sensitive to the entire history of the wall temperature distribution for hypersonic tunnel-wall boundary layers. Hence, by implication, the Crocco solution is not valid for hypersonic turbulent boundary layers unless both the wall temperature and pressure are nearly constant for essentially the entire history of the flow.

The purpose of the present Note is to show that on a flat plate where both the wall temperature and mean wall pressure are constant, neither of the limitations of parallel flow or of unity for the turbulent Prandtl number are required in order for the Crocco solution to apply to the turbulent boundary-layer flow. It is shown herein that this result is subject to restrictions on the magnitude of pressure fluctuations.

The same analysis is generalized to show that the compressible turbulent boundary layer on an isothermal swept flat plate is independent of the spanwise flow if the molecular Prandtl number is unity. The independence principle,[8–10] which for the present problem may be stated as simply $\bar{g} = \bar{F}$,[11] should then apply as a good approximation to the turbulent boundary layer on a swept flat plate for both incompressible flow with arbitrary Prandtl number and to compressible flow with unity Prandtl number. These results are again subject to restrictions on the magnitude of pressure fluctuation terms.

Analysis

To define the problem, the Reynolds averaged momentum and energy equations for turbulent boundary-layer flow on an infinite swept cylinder[10] are written in terms of the normalized mean profile variables $\bar{F}$, $\bar{g}$, and $\bar{\theta}$[12] and their corresponding fluctuating components.

Chordwise mean momentum equation

$$\bar{\rho}\bar{F}\frac{\partial \bar{F}}{\partial x}+\frac{\bar{\rho}\tilde{v}}{u_e}\frac{\partial \bar{F}}{\partial y} = -\frac{1}{u_e{}^2}\frac{\partial \bar{p}}{\partial x}-\frac{\bar{\rho}\bar{F}^2}{u_e}\frac{du_e}{dx}+\frac{1}{u_e}\frac{\partial}{\partial y}\left(\bar{\mu}\frac{\partial \bar{F}}{\partial y}-\overline{(\rho v)'F'}\right) \qquad (1)$$